Application Note

Biopharma

Agilent

Trusted Answers

Analysis of mRNA-Lipid Nanoparticles in Human Plasma using SEC-Static Dual-Angle Light Scattering and Refractive Index Detection

Authors

Brian Liau, Suresh Babu C.V., and Ravindra Gudihal
Agilent Technologies, Inc.

Li Zhang, Melgious Jin Yan Ang, and Yi Yan Yang
Bioprocessing Technology Institute

Introduction

In recent years, lipid nanoparticles have been used effectively for clinical delivery of siRNA, mRNA, and other nucleic acid payloads. As one of the breakthrough technologies to emerge from the COVID-19 pandemic, mRNA-loaded lipid nanoparticles (mRNA-LNPs) have been proven to be a safe and efficacious means of expressing proteins in human tissues without the potential for inducing genetic mutations. They are now being investigated for a variety of therapeutic applications beyond vaccination against infectious diseases, including oncology, personalized medicine, and rare genetic diseases.[1]

The stability of mRNA-LNPs in their storage buffers was of widespread interest during the pandemic because it was one of the primary determinants of vaccine shipping conditions, and therefore, the degree of logistical challenge faced during distribution. However, the stability of mRNA-LNPs in physiological fluids such as blood plasma is an equally important consideration when developing new drugs because it strongly influences the drug's efficacy, pharmacokinetics, and organ selectivity. The FDA guidance to industry on Biological Products that Contain Nanomaterials[2] reflects this, stating that "the impact of human plasma and blood on the stability of nanomaterials... should be examined".

In this application note, size exclusion chromatography (SEC) with online dual-angle light scattering and differential refractive index (RI) detection was used to characterize the reaction kinetics of mRNA-LNPs in human plasma. It was shown that the degradation kinetics of a widely used mRNA-LNP composition can be measured in real time by changes in hydrodynamic radius (R_h) and molecular weight (Mw).

The study shows that having an online, high-resolution SEC step greatly increases the power of light scattering analysis, as it eliminates interference from plasma components that typically confound bulk dynamic light scattering (DLS) analyses. In addition, as the technique profiles all particles in the sample without making implicit assumptions about the size of mRNA-LNPs, it is an ideal tool for the unbiased examination of the fate of mRNA-LNPs in complex media.

Experimental

Human plasma powder (P9523-5ML) and bovine serum albumin (A3782-5G) were purchased from Sigma-Aldrich.

Production of mRNA-LNPs

mRNA-LNPs were produced using the same composition as Comirnaty[1], the COVID-19 vaccine pioneered by Pfizer and BioNTech. mRNA was in vitro transcribed from a PCR-amplified dsDNA template, purified using spin columns (Monarch RNA cleanup kit, New England Biolabs), then dissolved in 1 mM sodium acetate buffer (pH 4.7) to form the aqueous phase. ALC-0315, ALC-0159, DSPC, and cholesterol were purchased from MedChemExpress and dissolved in ethanol at a molar ratio of 46.3:1.6:9.4:42.7 to form the organic phase. The lipid and mRNA solutions were allowed to undergo controlled mixing in a benchtop microfluidic device (NanoAssemblr Platform, Precision NanoSystems) with the organic phase and aqueous phase, at a volume ratio of 3:1. The total flow rate was 12 mL/minute and the N:P ratio was 6:1. The resulting mRNA-LNPs were buffer-exchanged into physiological saline solution and concentrated in ultracentrifuge tubes with a molecular weight cut-off (MWCO) of 30 K at 4 °C × 2,500 g × 60 minutes for a total lipid concentration of approximately 2.2 mg/mL. The formed LNPs were stored at 4 °C before being characterized by bulk DLS (Zetasizer, Malvern, UK) or the Agilent 1260 Infinity II Bio-SEC multidetector system.

mRNA-LNP plasma incubation

Human plasma powder was reconstituted in Milli-Q water according to the manufacturer's instructions, then centrifuged at 10,000 g for 10 minutes and filtered through a filter with a core size of 0.2 µm to remove particulates. Serum albumin was dissolved in 50 mM sodium phosphate buffer (pH 7.2) at a concentration of 40 mg/mL. mRNA-LNPs were diluted 1:10 (v:v) into either filtered plasma or serum albumin solution, then immediately injected at 15-minute intervals for SEC multidetector analysis.

Size exclusion chromatography and the Bio-SEC multidetector system

As shown in Figure 1, the following equipment stack was used:

- Agilent 1290 Infinity II Bio Flexible Pump (G7131A)
- Agilent 1290 Infinity II Bio Multisampler (G7137A)
- Agilent 1290 Infinity II Multicolumn Thermostat (G7116B) with Agilent InfinityLab Quick Connect Bio heat exchanger, standard flow (G7116-60071)
- Agilent 1290 Infinity II Diode Array Detector (G7117B) equipped with an Agilent InfinityLab Max-Light Cartridge Cell, 10 mm (G4212-60008)
- Agilent 1290 Infinity II Refractive Index Detector (G7162B)
- Agilent 1260 Infinity II Bio-SEC Multidetector System (G7805AA) featuring Bio-inert Static Dual-Angle and Dynamic Light Scattering Detector

Agilent 1260 Infinity II Bio-SEC Multidetector System (G7805AA)

Agilent Aquagel-OH Mixed-M 4.6 × 250 mm, 8 µm

Agilent 1290 Infinity II Bio LC System

Agilent 1290 Infinity II Diode Array (G7117B) and Refractive Index (G7162B) Detectors

Figure 1. Instrumentation and consumables.

Table 1. Agilent 1260 Infinity II Bio-SEC multidetector system parameters.

Chromatographic Conditions	
Mobile Phase	50 mM sodium phosphate, pH 7.2
Flow Rate	0.6 mL/min
Injection Volume	15 µL
Run Time	15 min
Thermostat Autosampler	5 °C
Temperature TCC	30 °C
LS Detector	30 °C, 5 Hz
System Calibration	
Concentration	10 mg/mL
dn/dc	0.186
Extinction Coefficient	0.66 mL/mg/cm
DLS Operational Parameters	
Correlator Run Time	5 s
Correlator Function Clip Time	10 µs
R^2	0.80
Eluent Viscosity	0.0079 p (viscosity of water at 30 °C)
Eluent Refractive Index	1.333 (refractive index of water)

The diode array detector was used primarily for system calibration and was not required for light scattering experiments. The quaternary pump was used in isocratic mode with only a single solvent line active to reduce baseline fluctuations in the RI detector. The Bio-SEC multidetector system was equipped to perform dual-angle light scattering at 15 and 90°, as well as dynamic light scattering. Two 4.6 × 250 mm PL aquagel-OH SEC columns with different molecular weight cutoffs, 500,000 Da (part number PL1549-5801) and 10,000,000 Da (part number PL1549-5800) were used for this study. Data acquisition and analysis was performed using Agilent Bio-SEC software (A.02.01).

Results and discussion

Analysis of mRNA-LNPs in phosphate buffer

mRNA-LNPs were fabricated using microfluidic technology and buffer-exchanged into 154 mM NaCl solution. They were diluted into 50 mM sodium phosphate buffer (pH 7.2) to a final lipid concentration of 0.22 mg/mL prior to analysis with either bulk DLS or the Bio-SEC multidetector system.

Figure 2 shows a representative SEC chromatogram. Baseline regions (blue shading) were carefully chosen, bracketing the region of interest (green shading) before each trace was individually checked for accurate baselining and integration. As the lipid-formed LNPs do not have strong UV chromophores, the RI detector was necessary for estimating the concentration of eluting analytes. Positive and negative deflections in the RI tracing away from the region of interest were attributed to dissolved air and salts in the injected sample. In the region of interest, the overlaid red dots indicate R_h measurements from the online DLS detector, and the thick blue line indicates Mw measurements from dual-angle light scattering.

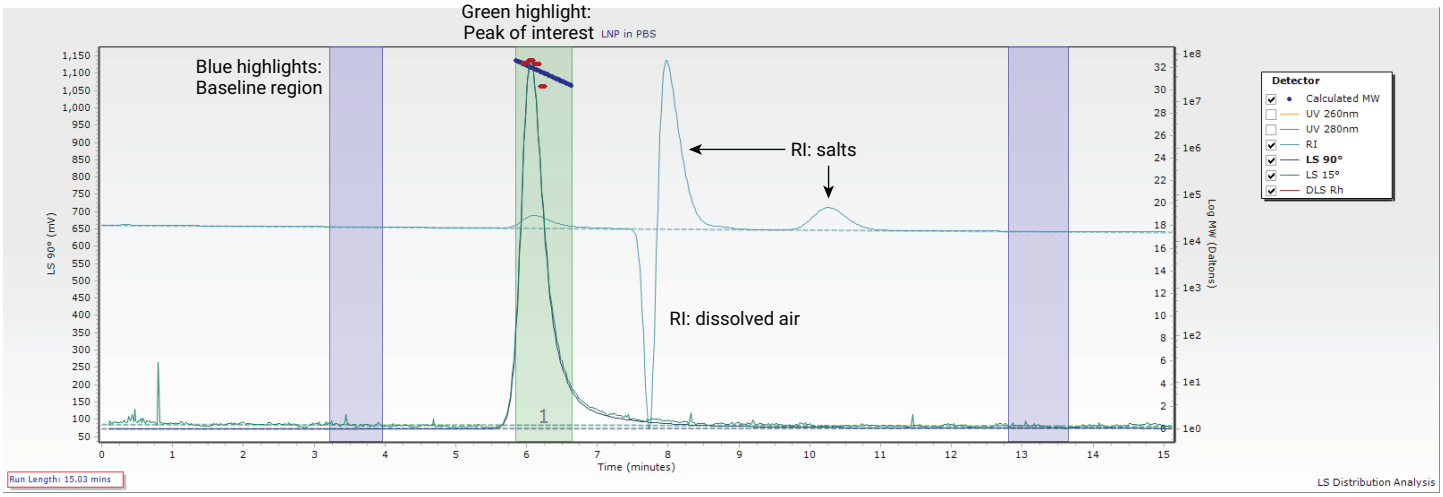

Figure 2. Representative SEC chromatogram.

As shown in Table 2, SEC multidetector R_h and polydispersity measurements showed excellent agreement with bulk DLS. As expected, both techniques showed the sample to be close to monodisperse. In addition, the Bio-SEC multidetector provided estimates of the sample Mw and radius of gyration (R_g) using static light scattering. These measurements, which are orthogonal to DLS, can be useful because they may indicate differences in particle composition that may not affect R_h, and may also yield insights into particle shape. In this case, R_g/R_h is approximately 0.9, which is close to the ideal value of 0.77 expected of monodisperse, compact spheres.

Chromatographic resolution of mRNA-LNPs and plasma components

As separation in SEC depends on the transient inclusion of analytes into porous chromatography resin, the resolution of analytes depends on both column length and pore size. In cases where a single column proves insufficient, two columns in series may provide superior resolution. In addition, columns with different pore sizes may be used to separate analytes over a wider range of molecular weights than can be addressed with a single type of column.

Figure 3 shows overlaid light scattering (LS90°) and refractive index chromatograms for mRNA-LNPs and human plasma

Table 2. Physical characteristics of mRNA-LNPs.

	R_h (nm)	Polydispersity*	Zeta Potential (mV)	R_g (nm)	Mw (MDa)
Bulk DLS	37.75	0.079	–0.47	–	–
Agilent 1260 Infinity II Bio-SEC multidetector system	31.94	1.017	–	28.87	43.1

* Polydispersity is calculated differently for DLS and the Agilent 1260 Infinity II Bio-SEC multidetector system. In DLS, the polydispersity index is scaled such that values < 0.05 are rarely seen other than with highly monodisperse standards, and values > 0.7 indicate a very broad size distribution. In dual-angle light scattering, polydispersity is defined as Mw/Mn.

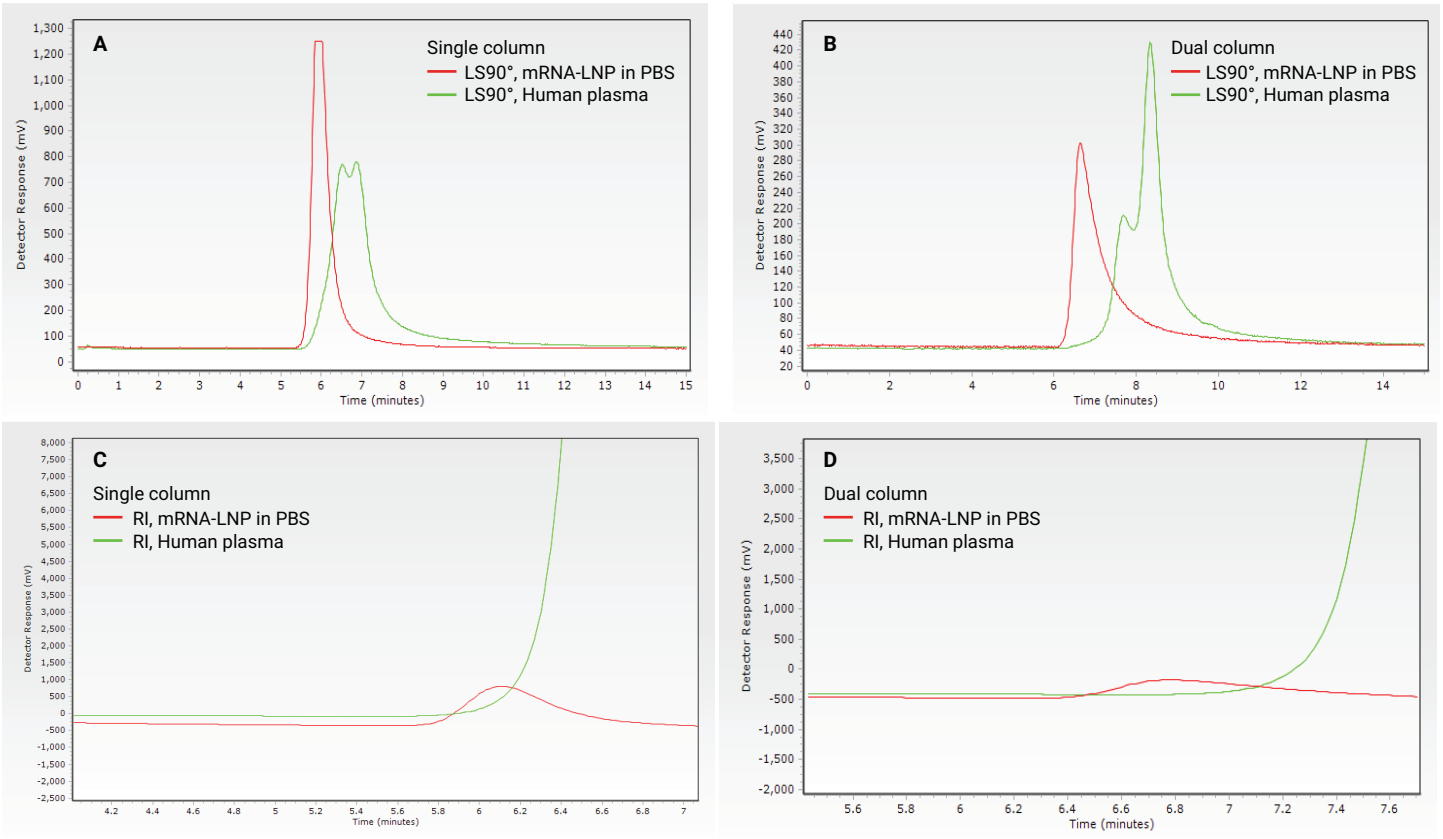

Figure 3. LS90° and refractive index chromatograms for mRNA-LNPs and human plasma injected separately onto single or dual-column SEC configurations.

injected separately in single or dual-column configurations. The single-column configuration comprised a wide pore 4.6 × 250 mm PL aquagel-OH column (10 MDa MWCO), and the dual-column configuration comprised the wide pore column followed by a second narrow pore 4.6 × 250 mm column (0.5 MDa MWCO).

Figure 3A clearly shows that the single-column configuration was unable to adequately resolve plasma components from mRNA-LNPs, whereas the dual-column configuration in Figure 3B provides acceptable resolution for much of the mRNA-LNPs' peak. In addition, the dual-column configuration resolves plasma components into two clear peaks, with the taller peak eluting at approximately 8.5 minutes, dominated by serum albumin (supporting data not shown). Figures 3C and 3D show that the RI signal attributable to mRNA-LNPs is much weaker than the LS90° signal and may easily be dominated by the much larger RI of the plasma components. Hence, good chromatographic separation (Figure 3D) is imperative for accurate determination of mRNA-LNPs Mw, since even minor coelution with plasma components can lead to large errors in mRNA-LNPs concentration estimates, thereby causing inaccurate Mw calculations.

Kinetics of mRNA-LNPs reaction with human plasma

Figure 4 shows mRNA-LNPs incubated in human plasma injected at 15-minute intervals and separated in a dual-column configuration. The LS90° chromatograms clearly show the mRNA-LNPs peak at 6.7 minutes decreasing in intensity over time, while the plasma component peak at 7.7 minutes increases correspondingly in intensity. Evidently, mRNA-LNPs are reacting with plasma components and decreasing in size, leading to an increase in retention time and coelution with plasma components at 7.7 minutes. Online DLS measurements (left inset) show that the R_h of plasma components in the 7.7-minute peak range from 12 to 16 nm; thus, the final size range of mRNA-LNPs after degradation can be inferred.

The inset figures on the right of Figure 4 show the futility of attempting to track this reaction using either the RI detector (Figure 4B) or via UV absorbance of the encapsulated mRNA at 260 nm using a diode array detector (Figure 4C). Due to its limited sensitivity, the RI detector shows only very small changes in the intensity of the peak attributable to mRNA-LNPs. These changes are more evident in the UV absorbance chromatogram. However, in both cases, the fate

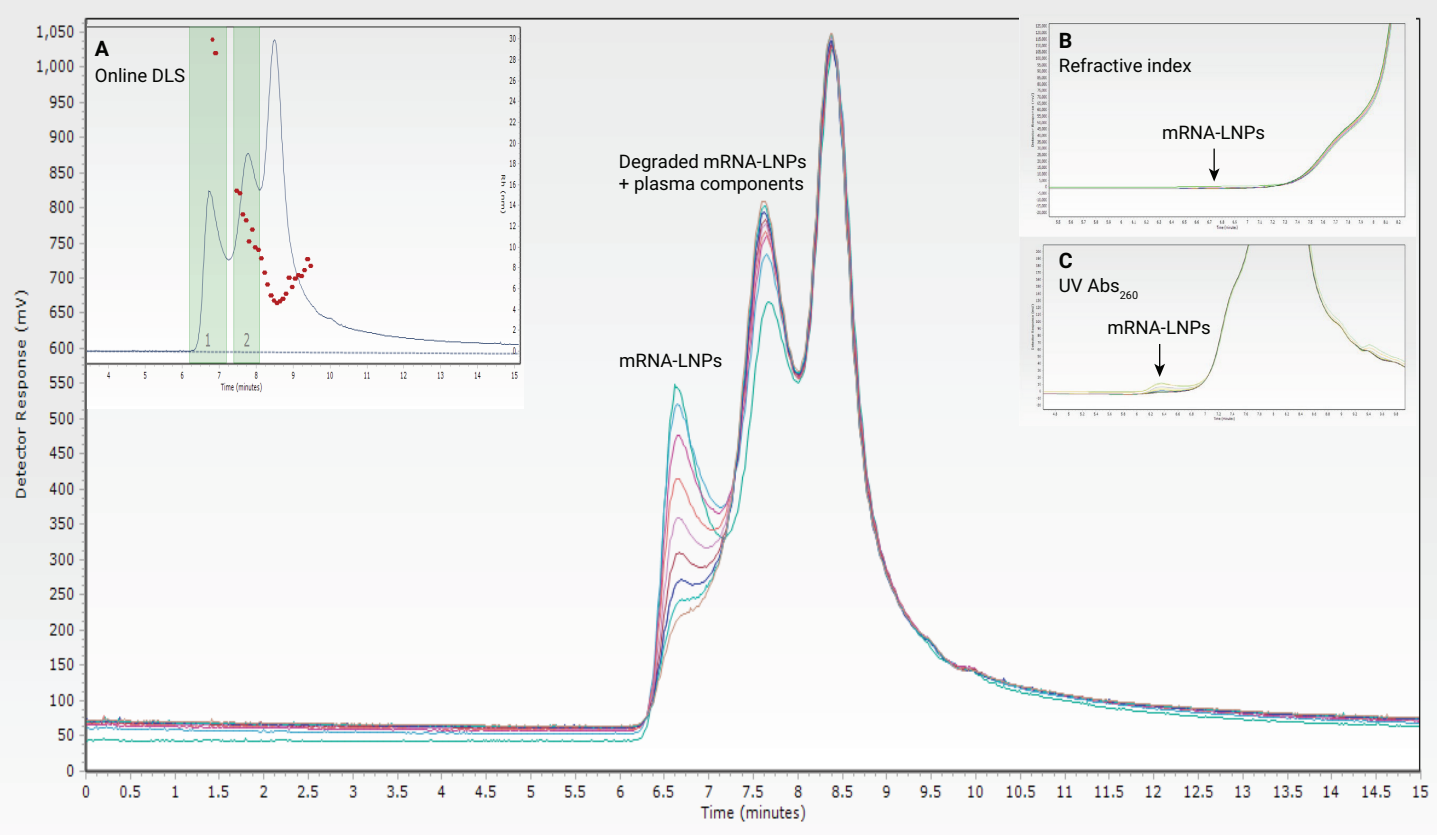

Figure 4. LS90° chromatograms of mRNA-LNPs incubated in human plasma over 120 minutes. (A) a representative trace showing online DLS measurements (red dots) across the three peaks. Refractive index (B) and UV absorbance (C) traces corresponding to the LS90° chromatograms.

of the mRNA-LNPs is unclear because the overwhelming signal from plasma components obscures where degraded mRNA-LNPs elute. Only the light scattering detector, with its higher sensitivity to particulate matter, is able to clearly make this determination.

Figure 5 shows the changes in the physical characteristics of the mRNA-LNPs peak over time. Figure 5A shows that the intensity of the peak decreases linearly with time, indicating that the reaction follows zero-order kinetics and is expected to go to completion in approximately 180 minutes. Figure 5B shows the average R_h of particles in the mRNA-LNPs peak, measured by online DLS. The average R_h falls from approximately 32 nm in sodium phosphate buffer to approximately 25 nm within 30 minutes of plasma incubation, providing direct evidence that the mRNA-LNPs are decreasing in size. Figure 5C corroborates this, as the apparent Mw of mRNA-LNPs decreases linearly with time. Figure 5D shows $M_{z+1} = \frac{\Sigma N_i M_i^4}{\Sigma N_i M_i^3}$ over time, which weights heavier particles much more than $Mw = \frac{\Sigma N_i M_i^2}{\Sigma N_i M_i}$. As shown, M_{z+1} remains approximately constant over time at approximately 40 MDa, which can be attributed to the signal from intact mRNA-LNPs. These data suggest that there is little to no increase in the size of mRNA-LNPs due to, e.g., protein coating, and that degradation is the dominant process.

In contrast, Figure 6 shows that mRNA-LNPs react with serum albumin, the most abundant component in blood plasma, very differently than with whole plasma. Figure 6A shows that the decrease in mRNA-LNP peak area is far more limited than in plasma and is not associated with any shift in retention time. Unlike in plasma, changes in peak area (Figure 6B) and Mw (Figure 6C) indicate that the reaction was completed within 30 minutes. There was no significant change in R_h, which averaged 29.8 ± 3.3 nm over the course of the experiment, whereas Mw increased from approximately 40 to 50 MDa after 30 minutes. Taken together, these data are consistent with a protein-coating process.

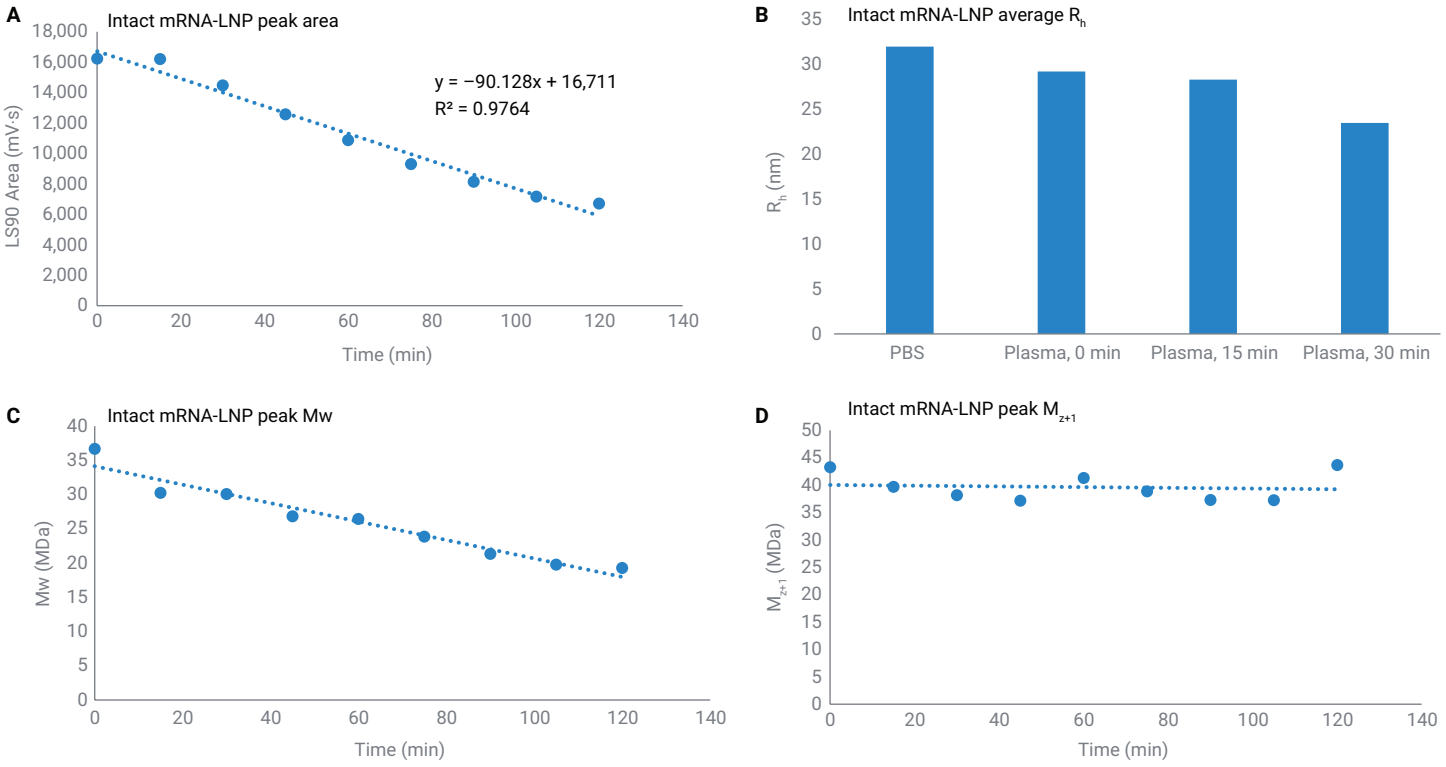

Figure 5. Physical characteristics of mRNA-LNPs incubated in human plasma as measured by online static dual-angle light scattering and DLS.

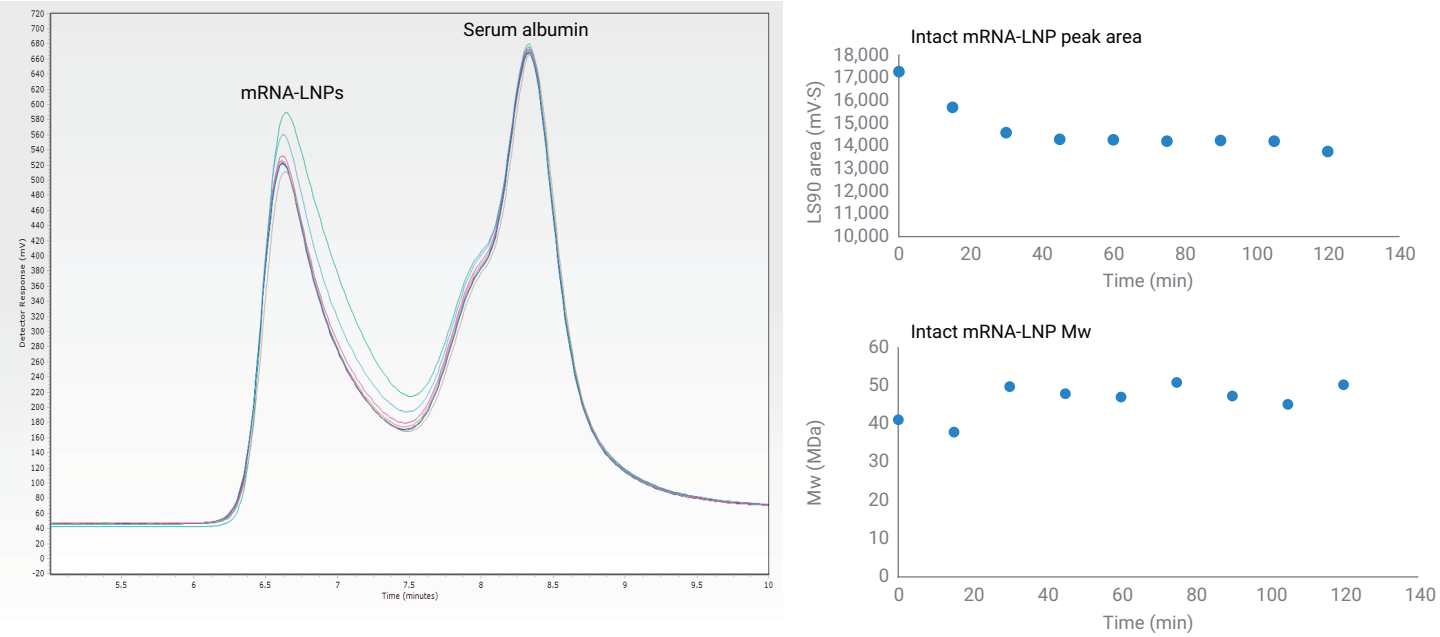

Figure 6. LS90° chromatogram and Mw of mRNA-LNPs incubated in serum albumin.

Conclusion

This study demonstrates the power of SEC with a multidetector system for the study of LNPs as: (i) it profiles all particles in a sample regardless of changes in size, (ii) it is far more sensitive to particulates than refractive index or UV absorbance detection, allowing nanoparticles to be detected even when obscured by sample matrix, (iii) SEC can eliminate interference from complex matrices such as plasma, facilitating accurate light scattering measurements, and (iv) it enables orthogonal determination of size and molecular weight through retention time, static, and dynamic light scattering in a single experiment, increasing experimental certainty.

References

1. Tenchov, R.; Bird, R.; Curtze, A. E.; Zhou, Q. Lipid Nanoparticles–From Liposomes to mRNA Vaccine Delivery, a Landscape of Research Diversity and Advancement. *ACS Nano* **2021**.
2. Drug Products, Including Biological Products, that Contain Nanomaterials – Guidance for Industry. *U.S. Food and Drug Administration*, April **2022**.

www.agilent.com

RA45250.5916550926

Printed in the USA, February 14, 2024
5994-6854EN

Agilent
Trusted Answers